buildings

MDPI

Article

Simplified Model of Heat Load Prediction and Its Application in Estimation of Building Envelope Thermal Performance

Ziyang Hao, Jingchao Xie *, Xiaojing Zhang and Jiaping Liu

Key Laboratory of Green Built Environment and Energy Efficient Technology, Beijing University of Technology, Beijing 100124, China; haozy@emails.bjut.edu.cn
* Correspondence: xiejc@bjut.edu.cn

Abstract: This study provides a reference for estimating the building envelope thermal performance at the initial stage of design for nearly zero-energy buildings in different climate zones. A simplified model of heat load prediction, which combines the quasi-steady-state thermal balance calculation procedure in ISO 52016 and the variable-base degree-days method, was proposed. Therefore, a building energy performance evaluation tool BPT V1.0 was developed. Subsequently, the simplified model was validated through comparative analysis with the Building Energy Simulation Test (BESTEST) standard procedure. To conduct a feasibility analysis of the development tool, case studies were performed on the performance evaluation of building envelopes of residential and office buildings in different climate zones in China. Compared to the simulation results from EnergyPlus, the deviation of heat load calculated by BPT V1.0 was within 10%, which further verifies the applicability of the tool under different climatic conditions. Annual heat load under different thermal performance building envelopes was calculated through BPT V1.0. The building energy efficiency improvement rates were found to range from 30 to 60% in nearly zero-energy buildings in different climate zones in China. The study results can provide a reference for energy managers and a basis for estimating the building energy efficiency performance with different envelope thermal properties in the region.

Keywords: heat load prediction; balance point temperature; quasi-steady-state method; variable-base degree-day; BESTEST

Citation: Hao, Z.; Xie, J.; Zhang, X.; Liu, J. Simplified Model of Heat Load Prediction and Its Application in Estimation of Building Envelope Thermal Performance. *Buildings* **2023**, *13*, 1076. https://doi.org/10.3390/buildings13041076

Academic Editors: Beatriz Arranz and Sergio Vega-Sánchez

Received: 5 March 2023
Revised: 10 April 2023
Accepted: 16 April 2023
Published: 19 April 2023

1. Introduction

Improvements in building energy efficiency can be achieved through active strategies, such as improving the performance of HVAC systems, lighting, and electrical equipment on one hand, and passive design strategies such as building envelope improvements [1], natural ventilation, and building shading on the other. With the continuous improvement of techniques, renewable energy technologies such as solar photovoltaic [2] or photothermal systems, and wind power have also been applied to buildings [3]. In recent years, the promulgation of technologies and standards for ultra-low energy buildings, nearly zero and zero energy buildings in various countries has revived significant interest in environmentally friendly passive building energy efficiency strategies [4]. In China, the 14th Five-Year Plan for Building Energy Conservation and Green Building Development issued by the Ministry of Housing and Urban–Rural Development in 2022 proposed that by 2025, ultra-low energy and nearly zero energy buildings (NZEBs) with an area of more than 50 million m^2 will be built [5]. An NZEB is defined as a building that has significantly high energy performance, requires little energy, and that energy is fully provided by energy from renewable sources, and has no on-site carbon emissions from fossil fuels [6]. High-performance passive house technologies are a prerequisite for the realization of NZEBs. Their features include better insulation and airtightness, high-efficiency windows, and passive solar gains. The buildings make efficient use of the sun, internal heat sources, and heat recovery, enabling the buildings to achieve a comfortable temperature that needs little

energy, without the help of conventional heating or air conditioning systems. The annual building heating energy should not be more than 15 kWh/m^2 or be designed with a peak heat load of 10 W/m^2 [7].

Proper building design and integration of high-performance envelopes [8] is the most effective way to reduce building energy demands [9] and provide occupants with thermal comfort. Compared to other solutions in buildings, the selection of envelope and materials is particularly important considering the long lifetime of the buildings and costs associated with the envelope. The International Energy Agency (IEA) states that more widespread and stringent building regulations, along with higher retrofit rates, have helped reduce space heating intensity (energy demand per total m^2) by an average of 10% globally over the past decade [10]. Therefore, improving the performance of the envelope [11] and reducing the heat gain/loss of the envelope is considered to be a key step in the design of NZEBs. This is also a primary consideration in the ongoing revision of building energy efficiency standards in various countries. Among them, the heat transfer coefficient of the envelope is a significantly important factor influencing the energy performance of a building [11–13]. Taking the *JGJ 26* series [14] in China as an example, from the *JGJ 26-86* promulgated in 1986 to the current *JGJ 26-2018* issued in 2018, compared with the benchmark buildings built in 1980, the energy-saving rates have increased from 30%, 50%, 65% to 75%, as shown in Figure 1. For the national standards *GB 55015-2021* [15] and *GB/T 51350-2019* [16], the requirements for building energy efficiency have been further increased. As energy efficiency requirements increase, more stringent requirements are imposed on building insulation performance, lowering the upper limit of the heat transfer coefficient of building envelopes. As listed in Table 1, taking Beijing as an example, prescriptive indicators such as the heat transfer coefficient of the building envelope and energy performance indicators have changed significantly at different stages over the past 30 years.

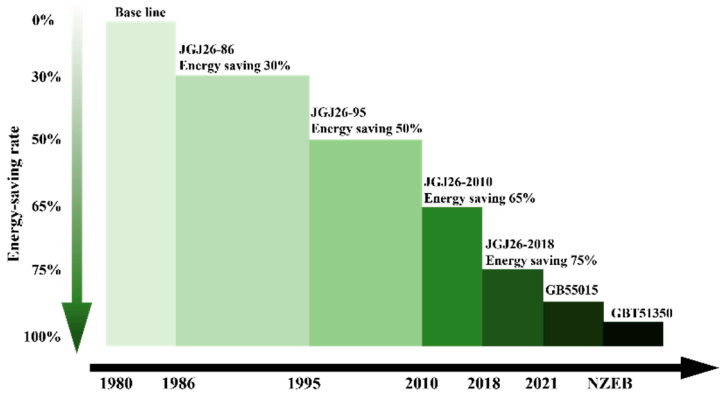

Figure 1. Improvements in energy efficiency in Chinese building standards.

Table 1. Comparison of series standards for energy-efficient design of residential buildings in Beijing.

	JGJ 26-86	JGJ 26-95	JGJ 26-2010	JGJ 26-2018	GB 55015-2021	GB/T 51350-2019
U_{wall}	1.61	0.9	0.60	0.45	0.45	0.1~0.3
U_{roof}	0.91	0.8	0.45	0.30	0.30	0.1~0.3
U_{window}	6.4	4.7	3.1	2.2	2.2	1.5
Energy performance indicator	Heat loss of building (W/m^2)			Annual heating loads (kW•h/(m^2•a))		
	25.3	20.6	15.0	≦23	≦18.61	≦15

Effective assessment of building energy performance uses quantitative indicators [17]. Several different energy performance indicators (EPI) [18] have been proposed to monitor and evaluate the energy performance of buildings and to gauge energy-saving rates under different building design strategies. Without considering renewable energy generation, the energy demand of a building is considered the aggregate energy performance indicator [19], which is the useful energy required to maintain comfort conditions and building functions;

it can be classified into energy demand for heating, cooling, domestic hot water, and lighting. The energy demand for heating or cooling is disaggregate energy performance indicators, considering the useful floor area of the building's habitable spaces that are generally expressed in kWh/m^2 year. Separate statistics, analysis, and management of sub-item energy use are conducive to a clear understanding of energy consumption by all subsystems of the building such that building energy conservation measures can be taken in a targeted manner. In northern China, the area north of the Qinling Mountains–Huaihe River Line has an extremely cold climate, and central heating systems of various sizes are widely used in northern cities and towns. National statistics show that heating energy demands contribute to 60% of the total energy consumption of residential buildings and 43% of public buildings in northern China. In areas south of this geographical line, the heating demand is also growing in some cities and the management of decentralized heating has not yet been supervised. Therefore, building heating in China has a large energy efficiency potential and accurate calculation of the annual heating demand is crucial to measure the energy performance of buildings. Therefore, in this study, the annual heating load of the building is chosen as the energy performance indicator, without considering the impact of heating system form and efficiency of the heating system.

In the early stages of building energy efficiency development in China, the steady-state calculation method of effective thermal transmittance was used to calculate the building heating energy loads [20], simplifying the outdoor temperature and solar radiation throughout the heating season into a fixed parameter to calculate the heating energy demand of different towns. This method is simple, and its calculation accuracy can meet the engineering requirements in the past when the building's thermal performance was not good. However, with the improvement in the thermal performance of the envelope, the steady-state calculation method is no longer suitable for calculating the current heating energy demand of new buildings [21]. There has been increasing literature on detailed full dynamic simulation tools in recent years [22–24], which are considered to be a suitable alternative reference approach to predict building energy demands for individual buildings, provided that there is sufficient information on all input data (including operating conditions) and their variations. Practically, however, such detailed full dynamic simulation tools introduce considerable choice, detail, and complexity, and rely heavily on the expertise of the operator [25]. The U.S. Department of Energy simulated building performance across the United States by surveying buildings across the country and using the building energy simulation software EnergyPlus. Based on this, benchmark building energy models representing realistic building characteristics, building practices, and energy use characteristics were extracted. For China, it is imperative to conduct nationwide building energy performance simulations. However, because of the varying climate conditions, complex building construction, and capital investment issues in China, the development of a building energy performance simulation tool that balances calculation accuracy and convenience is essential for assessing building energy performance. There exist two simplified methods for calculating heating energy needs available internationally. One is the utilization factor method (also known as the quasi-steady-state method) proposed by ISO 52016-1 [26], in which the monthly energy needed for heating is calculated as the difference between the monthly heat transfer through transmission and ventilation and the sum of the monthly gains from internal and solar sources multiplied by the gain utilization factor [27]. The other is the variable-base degree-day method [28], which calculates the balance point temperature of the building and heating degree-days based on it [29,30]. The balance point temperature [31] is the outdoor air temperature at which the heat gains owing to the internal sources and solar radiation are in balance with the heat losses through the building envelopes owing to temperature differences. The accumulation of the positive differences between the balance point and the outdoor temperatures is used to calculate the heat transfer through transmission and ventilation [28,32]. This study combines the above two methods, considers the thermal balance between the building and surrounding environment monthly [33], and uses the heat gain utilization factor to consider the dynamic effects. Combined with the definition

of building balance point temperature [34], the outdoor air-dry bulb temperature corresponding to zero monthly heating demand is taken as the balance point temperature. Then, with the calculated monthly heating balance point temperature as the base temperature, the monthly and annual heating loads of the building are determined through the variable-base degree-day method [35].

In Section 2, the heat load prediction model based on the new variable-base degree-day method was established, and a tool BPT V1.0 developed using the theoretical algorithm of the model was introduced. In Section 3, the accuracy of BPT V1.0 was verified using the state-of-the-art Building Energy Simulation Test (BESTEST) and Diagnostic Method procedures. Section 4 presents residential and office building models to evaluate the building envelope performance under different climatic conditions. The feasibility analysis of the BPT V1.0 tool was conducted by comparing the annual heating loads of representative cities in different climate zones with the simulation results of the standard tool EnergyPlus. Finally, according to the heat transfer coefficient value of the envelope under the prescriptive requirements of different energy efficient standards, we calculated the building balance point temperature and heating energy loads under the corresponding thermal engineering scheme, providing a reference for the building envelope thermal performance at the initial design stage of NZEBs in different climate zones.

2. Development of a Simplified Heat Load Model and Software

The proposed model in this study is applicable to a single thermal zone. The block diagram shown in Figure 2 reports the calculation procedure of the simplified heat load model and building energy simulation software BPT V1.0 based on it. Referring to the monthly calculation method in ISO 52016-1:2017, the thermal balance of the building is calculated at a monthly time interval. The input data considered by the BPT V1.0 software are geographical information of the building location (latitude, longitude, and time zone), typical climatic conditions (average dry-bulb air temperature, hourly global horizontal solar irradiance, and hourly direct normal solar irradiance), information relating to building's characteristics (such as building properties, occupancy loads and schedules, and indoor temperature set points). It handles the heat transfer through building envelope transmission and ventilation, heat gain from internal heat sources and solar heat gains through opaque and transparent envelopes, and heat gain utilization factor representing dynamic effects. The model does not consider thermal bridges or shadings. The main output results provided by this software program include monthly building balance point temperatures, monthly or annual heating degree days, and monthly or annual heat load for the whole building, as shown in Figure 2.

2.1. Calculation of Total Heat Transfer $Q_{ht;m}$

The total monthly heat transfer of a building comes from transmission and ventilation.

$$Q_{ht;m} = Q_{tr;m} + Q_{ve;m} \tag{1}$$

The monthly heat transfer by transmission, $Q_{tr;m}$, in kWh, is calculated as:

$$Q_{tr;m} = \left[H_{tr}(\theta_{int;H} - \theta_{e;m}) + H_{gr}(\theta_{int;H} - \theta_{e;an})\right]0.001\Delta t_m \tag{2}$$

$$H_{tr} = \sum_k (U_k \cdot A_k) + \sum_k (I_{tb;k} \cdot \psi_{tb;k}) \tag{3}$$

where H_{tr} is the overall transfer coefficient by transmission in W/K, for all building elements except those connected to the ground. U_k is the thermal transmittance for elements connected to the outdoor environment, in W/(m^2·K); A_k is the area of the building envelope element k, including walls, glazing, and roof, in m^2. $\sum_k (I_{tb;k} \cdot \psi_{tb;k})$ represents the heat transfer coefficient for thermal bridges, which is neglected in this research to preserve the simplicity of the calculation. H_{gr} is the ground heat transfer coefficient for building elements in thermal contact with the ground, and the detailed calculation of this part refers to ISO 13789:2017 [36]. $\theta_{int;H}$ is the heating setpoint temperature of the internal

environment, considering the space category and possible nighttime temperature set-back. $\theta_{e;m}$ and $\theta_{e;an}$ are the monthly and annual mean air temperature of the external environment, respectively. Δt_m is the duration of month m, in hours.

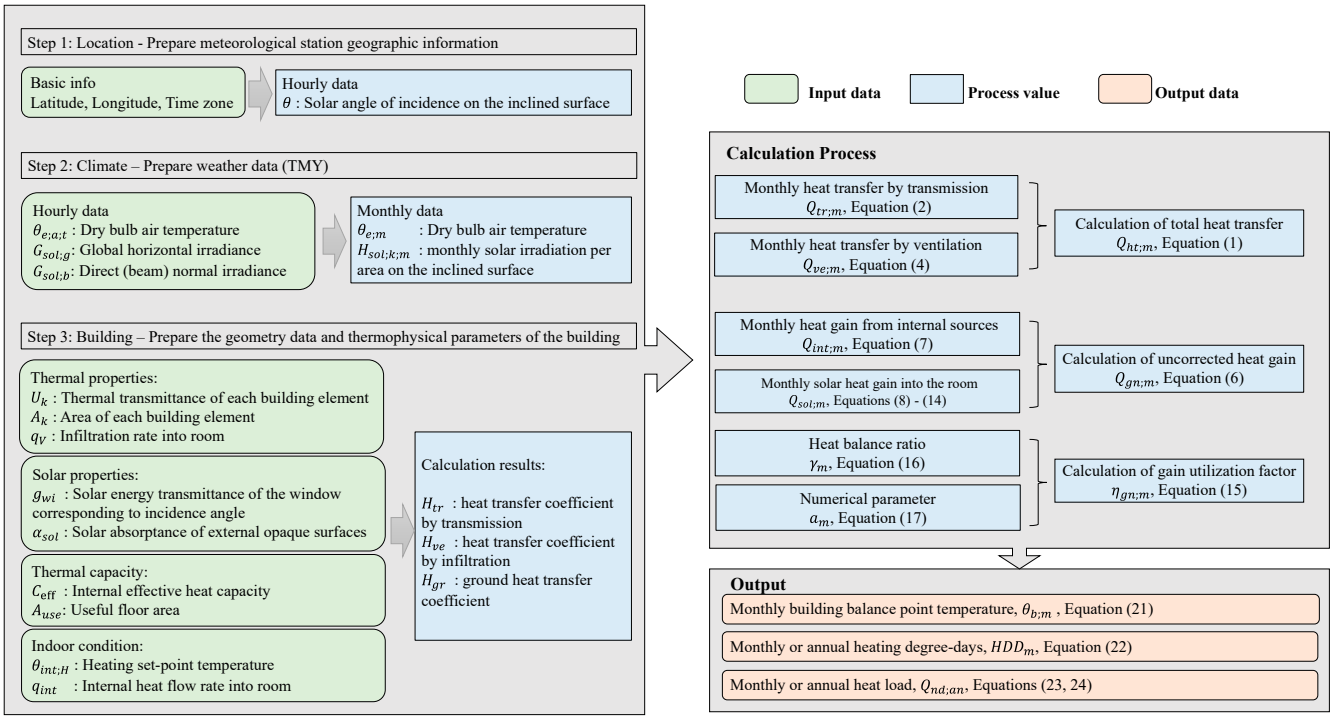

Figure 2. Calculation procedure of building energy simulation software BPT V1.0.

The total heat transfer by ventilation, $Q_{ve;m}$, in kWh, is calculated as:

$$Q_{ve;m} = H_{ve}(\theta_{int;H} - \theta_{e;m}) \cdot 0.001 \Delta t_m \quad (4)$$

$$H_{ve} = \rho_a c_a \sum\nolimits_k (q_{V,k}) \quad (5)$$

where $\rho_a c_a$ is the heat capacity of air per volume, in J/(m^3·K). H_{ve} is the heat transfer coefficient of the relevant airflow elements k, including air infiltration, natural ventilation, and mechanical ventilation, in W/K. Here, only infiltration is concerned, and it is estimated by the air change method, $q_V = ACH(V/3.6)$. The air change rate ACH (h^{-1}) and the volume of the heated space V (m^3) are considered.

2.2. Calculation of Uncorrected Heat Gains $Q_{gn;m}$

Uncorrected total monthly heat gain is calculated from internal and solar gains.

$$Q_{gn;m} = Q_{int;m} + Q_{sol;m} \quad (6)$$

The heat gain from internal heat sources of the building, $Q_{int;m}$, in kWh, for each month m, is calculated as follows:

$$Q_{int;m} = (q_{int;oc} + q_{int;A} + q_{int;L}) \times A_{use} \times 0.001 \Delta t_m \quad (7)$$

where the content in brackets refers to the specific internal heat flow rate due to metabolic heat from occupants, dissipated heat from appliances and lighting, in W/m^2; A_{use} is the useful floor area of the building, in m^2.

We determined the monthly amount of solar heat gains in the indoor environment, $Q_{sol;m}$, in kWh, for each element k, including opaque and glazing portions, and each orientation as follows:

$$Q_{sol;m} = Q_{sol;op;m} + Q_{sol;wi;m} = \sum_k Q_{sol;op;k;m} + \sum_k Q_{sol;wi;k;m} \quad (8)$$

$$Q_{sol;op;k;m} = \alpha_{sol;k} \cdot R_{se;k} \cdot U_k \cdot A_k \cdot F_{sh;obst;k;m} \cdot H_{sol;k;m} - Q_{sky;k;m} \quad (9)$$

where for each opaque element k, $\alpha_{sol;k}$ is the absorption coefficient for solar radiation; $R_{se;k}$ is the external surface heat resistance, in $m^2 \cdot K/W$, calculated from the exterior combined radiative and convective surface coefficient, $R_{se;k} = 1/(h_{ce;k} + h_{re;k})$. $F_{sh;obst;k;m}$ is the dimensionless shading reduction factor of external obstacles, which is considered to be 1 in this study. $H_{sol;k;m}$ is the monthly solar irradiation per area on the element k, which is expressed by the accumulation of hourly solar irradiance values, in kWh/m^2. $Q_{sky;k;m}$ is the monthly extra heat flow due to thermal radiation to the sky, in kWh, given by:

$$Q_{sky;k;m} = F_{sky;k} \cdot R_{se;k} \cdot U_k \cdot A_k \cdot h_{Ir;e;k} \cdot \Delta\theta_{sky;m} \cdot 0.001 \Delta t_m \quad (10)$$

where $F_{sky;k}$ is the view factor between the element k and the sky; $h_{Ir;e;k}$ is the external long-wave radiation heat transfer coefficient, in $W/(m^2 \cdot K)$; $\Delta\theta_{sky;m}$ is the average difference between the apparent sky and air temperatures based on Table B.31 in ISO 52016-1:2017. The default value is 13 K in the tropics, 11 K in the intermediate zones, and 9 K in the sub-polar areas.

As for the heat flow by solar gains through the transparent envelope element wi, $Q_{sol;wi;k;m}$, in kWh, is generally calculated using the following simplified formula:

$$Q_{sol;wi;k;m} = g_{wi;m} \cdot H_{sol;k;m} \cdot A_k \cdot \left(1 - F_{fr;wi}\right) - Q_{sky;k;m} \quad (11)$$

where $g_{wi;m}$ is the monthly mean effective total solar energy transmittance; $H_{sol;k;m}$ is monthly solar irradiation on the inclined surface, in kWh/m^2; and $F_{fr;wi}$ is the frame area fraction of the window. In this study, the influence of the shading reduction factor was not considered. Equation (11) uses the total solar energy transmittance $g_{wi;m}$ of the transparent part of the window, also known as the g-value, which is the ratio of energy passing through the window to the incident on the window. However, it is difficult to handle because the g-value of the glazing depends on the properties of the window and varies with the angle incidence of the radiation [37]. Considering that this angular dependence affects the solar radiation entering the building and thus, the energy demand, the g-value has to be described as precisely as possible for different incidence angles at different times. We adopted a polynomial empirical model [38,39] to express the g-value of direct and diffuse radiation as follows:

$$g_{wi,dir}(\theta) = g_o(\theta) \cdot \left[1 - a\left(\frac{\theta}{90}\right)^{\alpha} - b\left(\frac{\theta}{90}\right)^{\beta} - c\left(\frac{\theta}{90}\right)^{\gamma}\right] \quad (12)$$

where $a + b + c = 1$, $a = 8$, $b = 0.25/q$, $\alpha = 5.2 + 0.7q$, $\beta = 2$, $\gamma = (5.26 + 0.06p) + (0.73 + 0.14p)q$. p is the number of panes and q is the category parameter that depends on the coating type, which has been tabulated by Karlsson [38]. As a rule of thumb, the equivalent incidence angle of diffuse radiation was approximately 45°; therefore, the solar energy transmittance of glass for isotropic diffuse solar radiation can be calculated based on Equation (13).

$$g_{wi,dif} = g_o(45) \cdot \left[1 - a\left(\frac{45}{90}\right)^{\alpha} - b\left(\frac{45}{90}\right)^{\beta} - c\left(\frac{45}{90}\right)^{\gamma}\right] \quad (13)$$

Therefore, the transmitted solar irradiation $g_{wi;m} \cdot H_{sol;k;m}$ in Equation (11) should be calculated separately from the beam and diffuse components of the incident solar radiation. Then, Equation (11) can be expressed as:

$$Q_{sol;wi;k;m} = 0.001\left[\sum_{t_m}\left(I_{sol;dir;t} \cdot g_{wi,dir;t}(\theta) + I_{sol;dif;t} \cdot g_{wi,dif;t}\right)\right] \cdot A_k \cdot \left(1 - F_{fr;wi}\right) - Q_{sky;k;m} \quad (14)$$

where $I_{sol;dir;t}$ is the hourly value of the direct part of the solar irradiance on window wi, in W/m^2; $I_{sol;dif;t}$ is the hourly value of the diffuse part of the solar irradiance, in W/m^2, which includes diffuse sky irradiance and irradiance reflected from the ground.

2.3. Calculation of Gain Utilization Factor $\eta_{gn;m}$

In the quasi-steady-state monthly method, dynamic effects were considered by introducing a gain utilization factor for heating. The dimensionless heating gain utilization factor, $\eta_{gn;m}$, is a function of the heat/balance ratio for heating, γ_m, and the numerical parameter a_m, which depends on the inertia of the building. According to the formula in ISO 52016-1, the gain utilization factor for heating is calculated as follows:

$$\eta_{gn;m} = \begin{cases} \frac{1-(\gamma_m)^{a_m}}{1-(\gamma_m)^{a_m+1}}, \gamma_m > 0 \; and \; \gamma_m \neq 1 \\ \frac{a_m}{a_m+1}, \gamma_m = 1 \\ 1/\gamma_m, \gamma_m \leq 0 \; and \; Q_{gn;m} > 0 \\ 1, \gamma_m \leq 0 \; and \; Q_{gn;m} \leq 0 \end{cases} \quad (15)$$

$$\gamma_m = \frac{Q_{gn;m}}{Q_{ht;m}} \quad (16)$$

$$a_m = a_0 + \frac{\tau_m}{\tau_0} \quad (17)$$

where a_0 is the dimensionless reference numerical parameter, and the default value is 1.0; τ_0 is the reference time constant, and the default value is 15 h. τ_m is the time constant of the building in hours, characterizing the internal thermal inertia of the building.

$$\tau_m = \frac{C_{eff}/3600}{H_{tr} + H_{gr} + H_{ve}} \quad (18)$$

where C_{eff} is the effective internal heat capacity of the building, J/K. A simplified method [26] gives its default value as a function of the useful floor area A_{use}. The default values of internal heat capacity for different classes of construction types were taken from Table 2.

Table 2. Default values for internal effective heat capacity.

Class	$C_{m;eff}$ (J/K)
Very light	80,000 × A_{use}
Light	110,000 × A_{use}
Medium	165,000 × A_{use}
Heavy	260,000 × A_{use}
Very heavy	370,000 × A_{use}

2.4. Calculation of Heating Energy Demand

Based on the quasi-steady-state monthly method defined in ISO 52016-1:2017, the monthly energy needs for building heating can be calculated as

$$Q_{nd;m} = Q_{ht;m} - \eta_{gn;m} Q_{gn;m} \text{ (Provided that } 0 \leq \gamma_m \leq 2) \quad (19)$$

Substituting Equations (1), (2), (4), (6), and (8) into Equation (19) yields:

$$Q_{nd;m} = H_{tr}(\theta_{int;H} - \theta_{e;m})0.001\Delta t_m + H_{gr;an}(\theta_{int;H} - \theta_{e;an})0.001\Delta t_m + H_{ve}(\theta_{int;H} - \theta_{e;m})0.001\Delta t_m - \eta_{gn;m}\left(Q_{int;m} + Q_{sol;wi;m} + Q_{sol;op;m}\right) \quad (20)$$

Based on the concept of building balance point temperature [31], when the outdoor air condition is at the balance point temperature, a specific indoor air temperature can be maintained without the operation of any auxiliary heating system. Simply, when the monthly heating demand $Q_{nd;m}$ in Equation (20) is zero, the corresponding average outdoor air temperature $\theta_{e;m}$ is taken as the monthly building heating balance point temperature given by:

$$\theta_{b;m} = \theta_{int;H} - \frac{\eta_{gn;m}\left(Q_{int;m} + Q_{sol;wi;m} + Q_{sol;op;m}\right) - H_{gr;an}(\theta_{int;H} - \theta_{e;an})0.001\Delta t_m}{(H_{tr} + H_{ve})0.001\Delta t_m} \quad (21)$$

In this study, we used the monthly balance-point temperature as the variable base temperature for heating degree days [40,41]. Based on previous studies [33,42], the Hitchin' formula revised according to the local climate can accurately calculate the number of heating degree days in each month as follows:

$$HDD_m = \frac{N_m \times (\theta_{b;m} - \theta_{e;m})}{1 - exp[-k(\theta_{b;m} - \theta_{e;m})]} \quad (22)$$

where N_m is the number of days in a month. k is a location-specific constant given by $2.5/\sigma$, and σ is the standard deviation of the variation in temperature throughout the month.

The energy needed for building heating in a certain month and the whole year is estimated by the variable-based degree-day method [28].

$$Q_{nd;m} = 24 \times (H_{tr} + H_{ve}) \times HDD_m \quad (23)$$

$$Q_{nd;an} = \sum_{m=1}^{12} Q_{nd;m} \quad (24)$$

Considering the heat load is the amount of heat energy that needs to be added to a building to maintain a desired temperature setpoint, heating system effects are not considered in this calculation. Therefore, in the following, for the convenience of expression, the term heat load is adopted.

3. Model Validation Based on BESTEST

To check the credibility of the BPT V1.0 under certain operating conditions, we used the BESTEST (Building Energy Simulation Test) procedure to conduct a more detailed and authoritative verification and discussion of the simplified heat load prediction model [43]. The BESTEST is a standard method for testing and diagnosing building energy simulation programs that provide a set of standard procedure codes that are considered optimal for building energy performance analysis [44–46]. This method includes several test cases to evaluate the influence of different physical processes on the simulation results [47]. In this study, the selection of cases was based on the relevant parameters that are also considered in BPT V1.0. The selected cases are summarized in Table 3. The accuracy of the simplified model algorithm in Section 2 was evaluated by comparing the annual heating loads calculated by BPT V1.0 with the corresponding results obtained through the BESTEST procedures.

Table 3. Case Descriptions.

Case	Heating Setpoint, °C	Mass	Internal Gain, W	Infiltration, ach	External Shortwave Radiation Absorption	Glass m^2	Orientation
600	20	L	200	0.5	0.6	12	S
620	20	L	200	0.5	0.6	6,6	E, W
640	SETBACK	L	200	0.5	0.6	12	S
900	20	H	200	0.5	0.6	12	S
920	20	H	200	0.5	0.6	6,6	E, W
940	SETBACK	H	200	0.5	0.6	12	S
220	20	L	0	0	0.1	0	S
230	20	L	0	1	0.1	0	S
240	20	L	200	0	0.1	0	S
250	20	L	0	0	0.9	0	S
270	20	L	0	0	0.1	12	S
300	20	L	0	0	0.1	6,6	E, W

3.1. Base Building

The selected cases are based on a basic building model as shown in Figure 3. The reference building is a simple rectangular geometry with a single zone area of 48 m^2 and no interior partitions. It has a lightweight roof, floor, and walls, with a 12 m^2 south-facing window. All detailed material and thermal properties of the building envelope are provided in Table 4, referring to cases in ANSI/ASHRAE Standard 140-2017. The infiltration rate was set to 0.5 ach. The sensible heat generated internally was 200 W. The solar absorptance of the exterior opaque surface was 0.6. The exterior combined radiative and convective surface coefficient was 29.30 W/(m^2·K), and the interior combined radiative and convective surface coefficient was 8.29 W/(m^2·K). The thermostat heating setpoint temperature was set to 20 °C. The BESTEST procedures refer to the weather location of Denver (CO, USA), and its weather data file type is TMY1.

Table 4. Materials and thermophysical parameters of the low-mass and high-mass cases.

Structure	Thickness (m)	R (m^2·K/W)	Density (kg/m^3)	c_p J/(kg·K)	Structure	Thickness (m)	R (m^2·K/W)	Density (kg/m^3)	c_p J/(kg·K)
Low-mass case (Case 600): External wall					High-mass case (Case 900): External wall				
Interior surface coefficient h_o = 8.290 W/(m^2·K)					Interior surface coefficient h_o = 8.290 W/(m^2·K)				
Plasterboard	0.012	0.075	950	840	Concrete block	0.100	0.196	1400	1000
Fiberglass quilt	0.066	1.650	12	840	Foam insulation	0.0615	1.537	10	1400
Wood siding	0.009	0.064	530	900	Wood siding	0.009	0.064	530	900
Exterior surface coefficient h_o = 29.30 W/(m^2·K)					Exterior surface coefficient h_o = 29.30 W/(m^2·K)				
U value: 0.514 W/(m^2·K)					U value: 0.512 W/(m^2·K)				
Low-mass case: Floor (inside to outside)					High-mass case: Floor (inside to outside)				
Interior surface coefficient h_i = 8.290					Interior surface coefficient h_i = 8.290				
Timber flooring	0.025	0.179	6500	1200	Concrete slab	0.080	0.071	1400	1000
Insulation	1.003	25.075	0	0	Insulation	1.007	25.175	0	0
U value: 0.039 W/(m^2·K)					U value: 0.039 W/(m^2·K)				
Low-mass case: Roof (inside to outside)					High-mass case: Roof (inside to outside)				
Interior surface coefficient h_i = 8.290					Interior surface coefficient h_i = 8.290				
Plasterboard	0.010	0.063	950	840	Plasterboard	0.010	0.063	950	840
Fiberglass quilt	0.1118	2.794	12	840	Fiberglass quilt	0.1118	2.794	12	840
Roof deck	0.019	0.136	530	900	Roof deck	0.019	0.136	530	900
Exterior surface coefficient h_o = 29.300					Exterior surface coefficient h_o = 29.300				
U value: 0.318 W/(m^2·K)					U value: 0.318 W/(m^2·K)				
Window properties (double-pane uncoated glass)									
U-value					3.0 W/(m^2·K)				
Double-pane shading coefficient (at normal incidence)					0.907				
Double-pane solar heat gain coefficient (at normal incidence)					0.789				

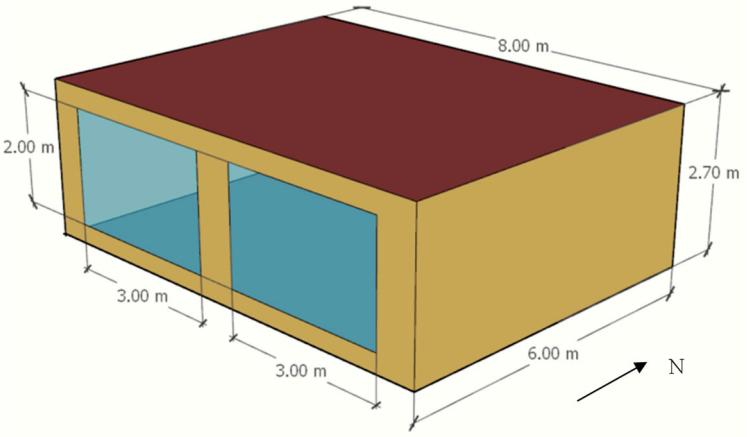

Figure 3. Geometry of the test room.

3.2. Basic Cases and In-Depth Cases

The basic tests analyze the ability of BPT V1.0 to simulate building envelope loads in low- and high-mass configurations, respectively. The low-mass basic tests are cases 600, 620, and 640, as described in Table 3. Case 600 is completely consistent with the base building model described in Section 3.1. Case 620 is modeled the same as Case 600 except for the change in window orientation, which is modified to have 6 m^2 of window area facing east and 6 m^2 of window area facing west. Case 640 is modeled the same as Case 600 except for changes in the thermostat control strategy. The thermostat's heating temperature is set to 20 °C from 07:00 to 23:00 and 10 °C for the rest of the time. The high-mass basic tests are cases 900, 920, and 940, which are modeled the same as the corresponding low-mass series (600, 620, and 640), except that the material and thermal properties were taken from the right side of Table 4 instead of the left side. The overall heat transmission coefficient was equivalent in both the high-mass and low-mass cases such that the sensitivity to thermal mass could be assessed under several parametric variations.

The in-depth test cases are modeled as detailed in Table 3, which are Cases 220, 230, 240, 250, 270, and 300, to provide detailed diagnostic capability by stimulating specific heat transfer mechanisms to analyze the effects of different physical phenomena on building energy results [44,48]. Case 220 is the base case of the in-depth series and is modeled the same as the base building in Section 3.1 except for the changes specified in the following description. It is modeled as an enclosed space with an infiltration rate of zero, no internal heat gain, and the solar absorptance of the external opaque enclosure was set to 0.1. The 12 m^2 transparent window on the south wall was replaced by an opaque window element with a shortwave transmittance of zero and a solar absorptance of 0.1. Then, based on the model descriptions of Cases 240, 250, 270, and 330 provided in Table 3, the simulation parameters considered in the algorithm were progressively modified to test the calculation codes in BPT V1.0 related to infiltration, internal gains, exterior solar absorptance, south solar gains, and window orientation. Subsequently, the sensitivity of the algorithms was tested by comparing the differences in heat load caused by parameter modification.

3.3. Comparative Tests and Sensitive Analysis

Based on the diagnostic logic of the test cases, the results calculated by BPT V1.0 were compared with the output data of the reference code in BESTEST at each stage to show the reliability of BPT V1.0. The reference results obtained from the standard codes provided in the BESTEST procedure delineate the confidence intervals within which the results obtained with BPT V1.0 should be included. As the heat gain from solar radiation through transparent windows has a considerable influence on heating loads, the annual incident and transmitted solar radiation in different orientations calculated by BPT V1.0 and other BESTEST procedures were compared. From Table 5, the results calculated by

BPT V1.0 are included in the range of values obtained by the validation tests considered in the BESTEST procedure.

Table 5. Annual incident/transmitted solar radiation and annual transmissivity coefficient of windows.

	Annual Incident Solar Radiation (kWh/m^2)		Annual Transmitted Solar Radiation (kWh/m^2)		Annual Transmissivity Coefficient of Windows	
	Confidence Interval	**BPT V1.0**	**Confidence Interval**	**BPT V1.0**	**Confidence Interval**	**BPT V1.0**
North	367~457	430				
East	959~1217	1150				
West	857~1090	1047	563~735	693	0.641~0.687	0.662
South	1456~1566	1547	914~1051	993	0.623~0.671	0.642
Horizontal	1797~1832	1849				

Here, we compared the results of the developed tool BPT V1.0 with those of standard simulation tools provided in BESTEST. Figure 4 shows the simulation results of the annual heating loads for a set of test cases (low-mass 600-series and high-mass 900-series) conducted by the BESTEST procedure. The horizontal bands delimiting reference ranges are superimposed on the results to allow a comparison of the BPT V1.0 with these results. From Figure 4, the results obtained using the BPT V1.0 are included in the confidence interval allowed by the considered validation test. It was shown that the result is in good agreement with previous standard simulation tools for heating load calculations. In Figure 5, the heat load of the investigated building models in the in-depth test cases is reported. Clearly from the figure, the output from BPT V1.0 has a satisfactory consistency with the results obtained by the other standard procedures.

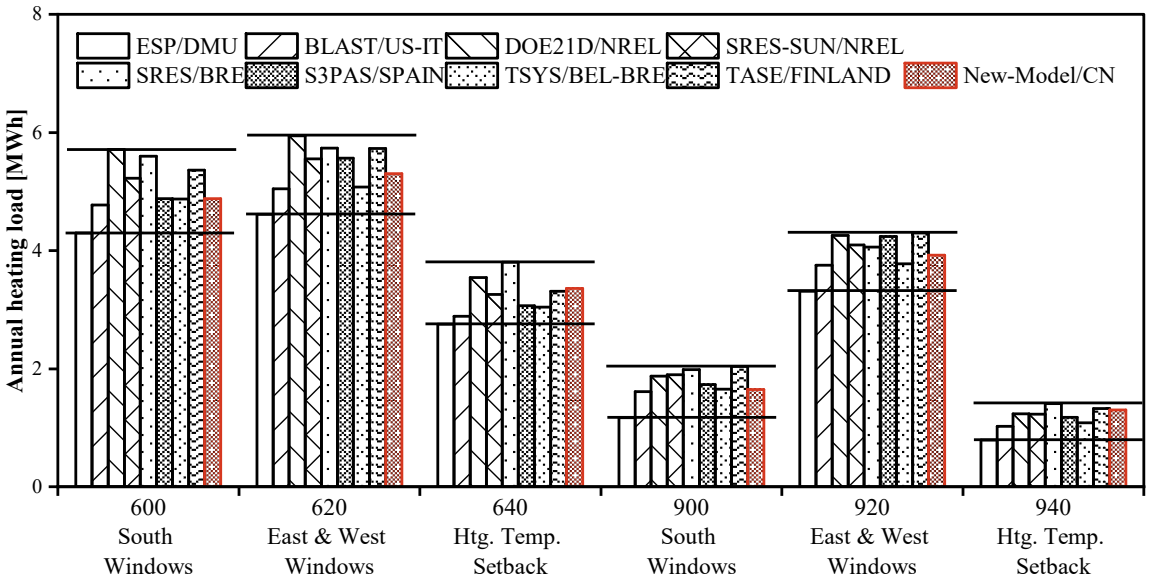

Figure 4. Annual heating load for low-mass 600-series and high-mass 900-series.

A further sensitivity analysis was performed for each parameter of BPT V1.0 through diagnostic tests. The annual heat load difference of BPT V1.0 caused by a single parameter change was compared with that of the standard simulation codes to verify the sensitivity of BPT V1.0 to different parameters. These diagnostic tests in Table 6 list the features tested, thus indicating potential sources of variance in the BPT V1.0 algorithmic. Clearly from the table, the direction of sensitivity of BPT V1.0 to the differences in heat load results between these cases is consistent, and the magnitude of the differences is also within an acceptable range. Taking Case 620-Case 600 in Table 6 as an example, the heat load differences obtained from the BESTEST procedure range from 0.138 to 0.682 MWh/year, and the load difference calculated by BPT V1.0 is 0.562 MWh/year, within the above range.

Combining the results of comparative tests and sensitivity analysis, it can be seen that BPT V1.0 has a good response to the above-mentioned parameters in terms of heat load calculation results.

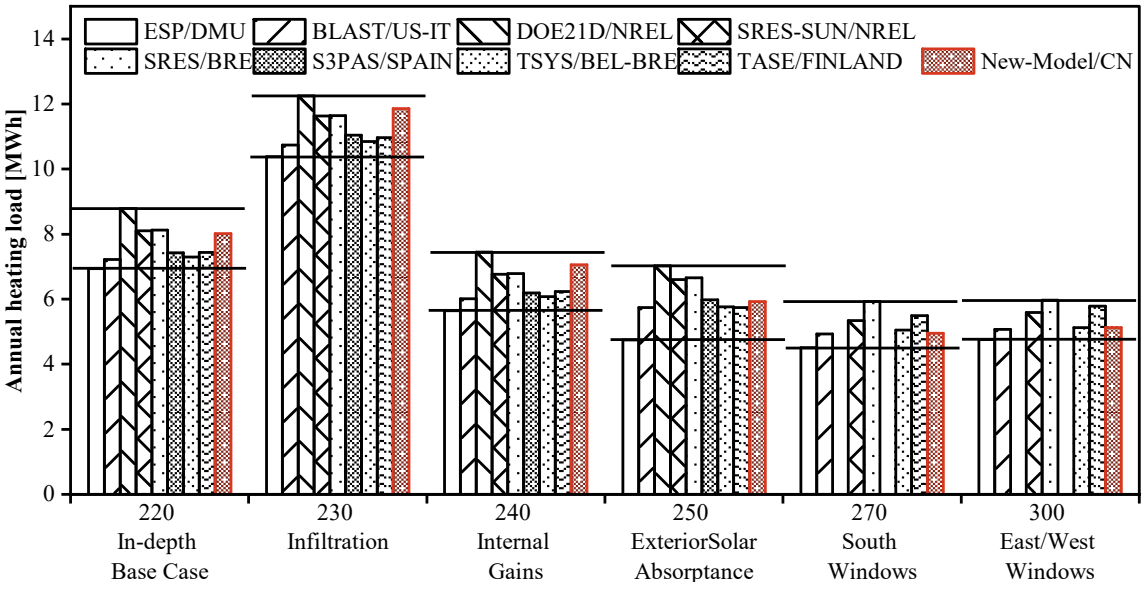

Figure 5. Annual heating load for in-depth test cases.

Table 6. Diagnostic tests and sensitivity analysis.

Cases	Diagnostic Tests	Heat Load Differences (MWh/y)		
		Min	Max	BPT V1.0
600	Base building			
620	620-600 test east and west solar transmittance/incidence	0.138	0.682	0.562
640	640-600 test night setback	−2.166	−1.545	−1.577
900	900-600 test thermal mass and solar interaction	−3.837	−3.126	−3.246
920	920-900 test east and west transmittance/mass interaction	2.070	2.505	2.278
940	940-900 test setback/mass interaction	−0.718	−0.377	−0.380
220	In-Depth Base Case			
230	230-220 test infiltration	3.432	3.615	3.597
240	240-220 test internal gains	−1.341	−1.203	−1.211
250	250-220 test exterior Shortwave Absorptance	−2.193	−1.448	−2.079
270	270-220 test south solar transmittance/incident solar	−2.761	−1.948	−2.755
300	300-270 test east and west solar transmittance and incidence	0.044	0.297	0.172

4. Feasibility Analysis of the Developed Tool

In Section 3, the accuracy and sensitivity of the BPT V1.0 algorithm code for predicting annual heat loads are verified based on Denver weather data and simple geometry using the BESTEST procedure. Nevertheless, some studies [43,49–51] have pointed out that when developing energy needs calculation software, it is necessary to analyze the calculation capacity of the actual whole building under different climatic conditions to clarify the feasibility of the developed model. Therefore, this section conducts case studies of residential and office buildings with different envelope performances in different climate zones in China. Further analysis was conducted by comparing the heating loads obtained from BPT V1.0 and the recognized standard simulation tool EnergyPlus [52,53].

4.1. Weather Stations in Different Climate Zones

There are five climate zones in China for building thermal design purposes, among which the regions with heating demand are severe cold zone (with three subdivisions: 1A, 1B, and 1C), cold zone (with two subdivisions: 2A and 2B), and hot summer and cold

winter zone (with two subdivisions: 3A and 3B). To analyze the adaptability of BPT V1.0 to different climates, 381 weather locations with different weather characteristics from 1A to 3B were selected. The geographic locations of the selected cities are shown in Figure 6, with different climate zones marked with different colors. Further, representative cities from different climate zones were selected for a detailed comparative analysis of heat load results. The selection results are reported in Table 7, with HDD18 ranging from 7994 K·d in Mohe to 959 K·d in Guilin, in descending order of HDD. In the same table, the latitude and longitude of the surveyed sites, the temperature of the coldest and hottest months, and the annual incident solar radiation (ISR) on the horizontal surface are also reported. According to the calculation flow chart in Figure 2, the required meteorological parameters in the input data are mainly outdoor air dry-bulb temperature and solar irradiation data. Concerning the selected weather data [54], the Typical Meteorological Year (TMY) data file in the JGJ/T346-2014 [55] of China was considered. Here, all the input meteorological data, such as air dry-bulb temperature and solar radiation, changed based on hourly profiles.

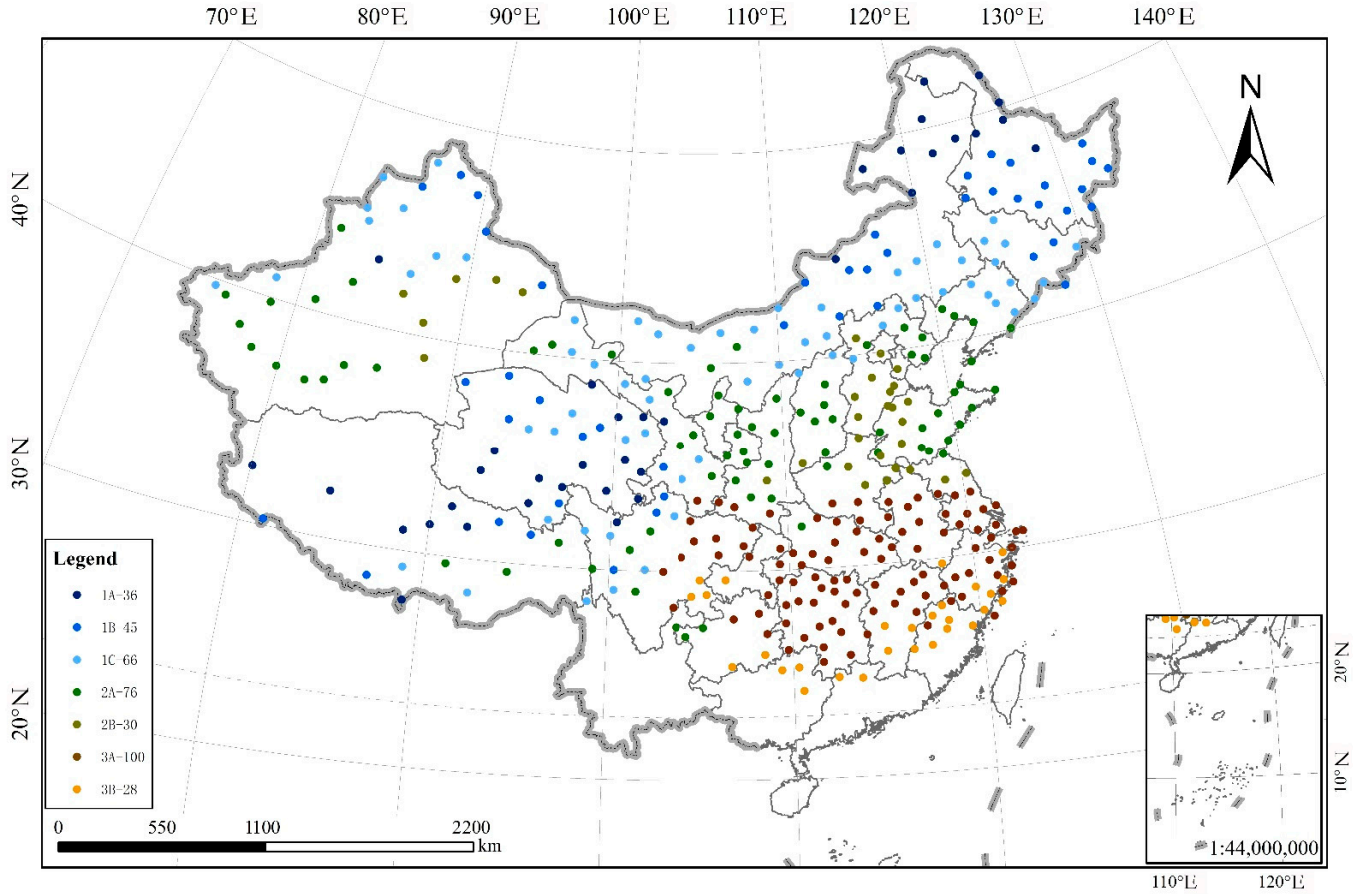

Figure 6. Geographic locations of the selected cities.

Table 7. Climate zones, representative cities, and related weather indexes.

Stations	Climate Zones	Longitude (°E)	Latitude (°N)	$T_{min,m}$ (°C)	$T_{max,m}$ (°C)	HDD18 (K·d)	ISR (kWh/m^2·y)
Mohe	1A	122.52	52.13	−28.4	18.6	7994	1136
Harbin	1B	126.77	45.75	−16.9	23.8	5032	1327
Hohhot	1C	111.68	40.82	−10.8	23.4	4186	1640
Dalian	2A	121.63	38.90	−3.4	24.1	2924	1402
Beijing	2B	116.28	39.93	−2.9	27.1	2699	1457
Shanghai	3A	121.43	31.17	4.9	28.5	1540	1380
Guilin	3B	110.30	25.32	8.7	28.0	989	1234

4.2. Building Models with Different Thermal Performance

To analyze the impact of building properties and operating conditions on the results of the BPT V1.0, residential and office buildings were selected. The benchmark building models are shown in Figure 7. The choice of these two different building typologies was based on considerations of different shape coefficients, window-to-wall ratios, infiltration rates, and internal heat source usage. The simulation assumptions for the building models are presented in Table 8. The indoor infiltration rate of the office building was based on a minimum fresh air demand of 30 cubic meters per person per hour. The internal load schedules shown in Figure 8, including electric equipment, lighting, and occupant, were selected based on the typical Chinese standard for the chosen building type. The envelope stratification of the benchmark buildings simulated here refers to the typical building structure of China in the 1980s, as shown in Table 9.

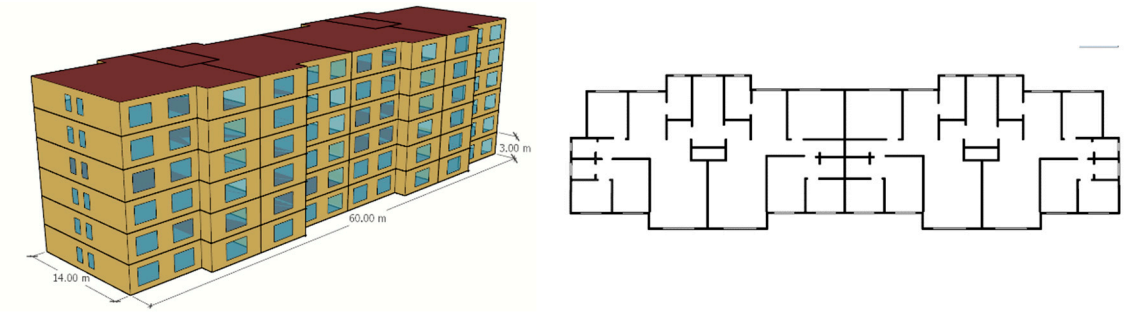

(**a**)

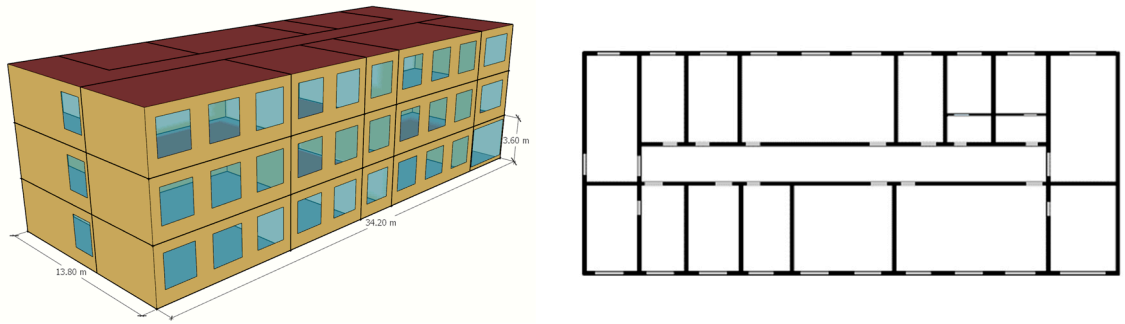

(**b**)

Figure 7. Simulated buildings models and typical floor plans (**a**) residential building; (**b**) office building.

Table 8. Simulation assumptions.

Descriptions		Residential Building	Office Building
Absorptance of an opaque exterior surface		0.6	0.6
Solar Heat Gain Coefficient		0.65	0.65
Shape coefficient		0.23	0.30
Infiltration rate—Air changes (h^{-1})		0.5	0.831 [1]
Window-to-wall ratio (%): S/N/E/W		0.3/0.25/0.05/0.05	0.40/0.35/0.08/0.08
Internal sensible heat gains	Average floor area per capita (m^2)	25	10
	Average occupancy rate	0.44	0.39
	Equipment power density (W/m^2)	3.8	13
	Average equipment usage rate	0.17	0.37
	Lighting power density (W/m^2)	5	9
	Average lighting usage rate	0.15	0.39
	Equivalent value input into BPT V1.0 (W/m^2)	2.36	10.40

[1] Calculated based on per capita fresh air volume of 30.

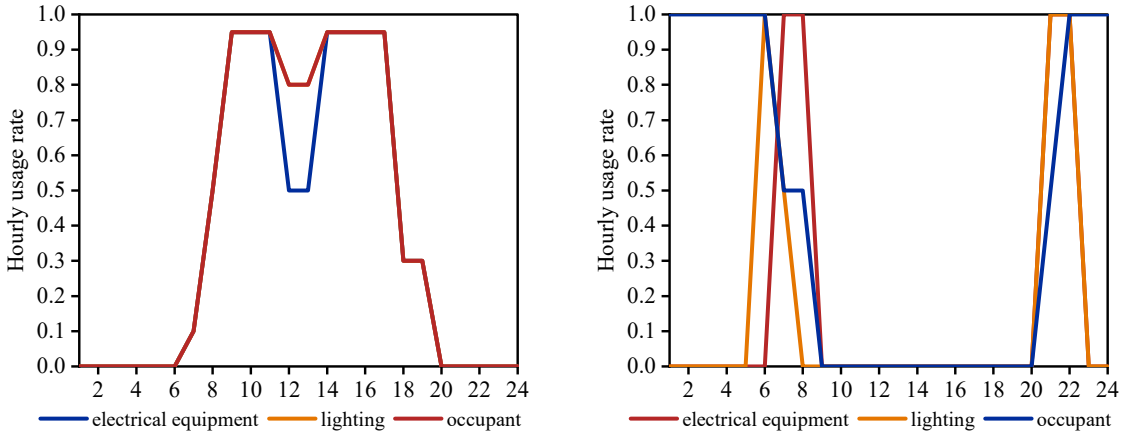

(**a**) [1] (**b**)

Figure 8. Overview of the building occupancy schedules: (**a**) office building; and (**b**) residential building. [1] "occupant" schedule curve coincides with the "lighting" of the office building.

Table 9. Envelope and thermal properties of the simulated building.

Building Elements	Heat Transfer Coefficient W/(m^2·K)	Envelope Stratification (from Inside to Outside)
Wall	0.87	Plasterboard (20 mm) + Aerated Concrete (200 mm) + Plaster (20 mm)
Roof	0.90	Plasterboard (20 mm) + Aerated Concrete (200 mm) + Roof deck (20 mm)
Floor	0.47	Terrazzo block (50 mm) + XPS Floor Insulation (80 mm) + Reinforced Concrete (100 mm) + Plasterboard (20 mm)
Window	3.23	

To explore the influence of thermophysical parameters of building envelopes stipulated in different building standards on heating loads, this study refers to [15,16]. According to the technical parameter requirements of the residential and public building envelope specified in these standards, the average heat transfer coefficients of envelopes in different climate zones are selected based on the values in Table 10. The smaller the upper limit values of the heat transfer coefficient, the better the thermal performance.

Table 10. Upper limits of envelope heat transfer coefficient for office and residential buildings in different climate zones under different standards.

Climatic Zones		Residential Building										
		1A	1B	1C	2A	2B	3A	3B	4A	4B	5A	5B
Energy-saving building	U_{wall}	0.35	0.35	0.40	0.45	0.45	1.00	1.20	1.5	1.5	1.0	1.0
	U_{roof}	0.15	0.20	0.20	0.25	0.30	0.40	0.40	0.4	0.4	0.4	1.8
	U_{window}	1.60	1.80	2.00	2.20	2.20	2.80	2.80	3.00	3.50	2.50	4.0
NZEB	U_{wall}	0.10~0.15			0.15~0.20		0.15~0.40		0.30~0.80		0.20~0.80	
	U_{roof}	0.10~0.15			0.10~0.20		0.15~0.35		0.25~0.40		0.20~0.40	
	U_{window}	1.0			1.2		2.0		2.5		2.0	

Climatic Zones		Office Building					
		1A/1B	1C	2A/2B	3A/3B	4A/4B	5A
Energy-saving building	U_{wall}	0.35	0.38	0.5	0.8	1.5	1.5
	U_{roof}	0.25	0.3	0.4	0.4	0.4	0.8
	U_{window}	2.3	2.4	2.5	2.6	3.0	4.0
NZEB	U_{wall}	0.1~0.25		0.1~0.3	0.15~0.4	0.3~0.8	0.2~0.8
	U_{roof}	0.1~0.2		0.1~0.3	0.15~0.35	0.3~0.6	0.2~0.6
	U_{window}	1.2		1.5	2.2	2.8	2.2

4.3. Validation of BPT V1.0 by Means of EnergyPlus

In the section, the annual heating loads of residential and office buildings in representative cities from different climate zones calculated by BPT V1.0 were compared with the corresponding results obtained by the standard simulation tool EnergyPlus, which is a good representation of the state-of-the-art of the BESTEST procedure.

Figure 9 shows the annual heating loads for all case studies. Within each pair of comparisons, the percent deviation of the results is reported at the end of the stacked bars. As observed from the figure, the deviations of the BPT V1.0 results vs. the EnergyPlus ones (considered as reference) are often less than 10% for representative cities in climate zones 1A to 3B. From the obtained data, it is clear that the software developed in this study has good adaptability to heat load prediction under different climate conditions. Comparing the heat load results in deviations of residential and office buildings (between BPT V1.0 and EnergyPlus), it can be concluded that for office buildings with large window-to-wall ratio, large air infiltration, and high internal heat gain, the calculation deviation is relatively large, but it is still within the acceptable deviation range of 10%. This is an important finding in understanding the feasibility of the model developed in this study for different types of buildings under different climatic conditions. The obtained conclusion of annual heat loads of different cities can be used as reliable energy performance indicators for energy managers. Future work will perform more rigorous calculations of each component of the heat load in actual buildings.

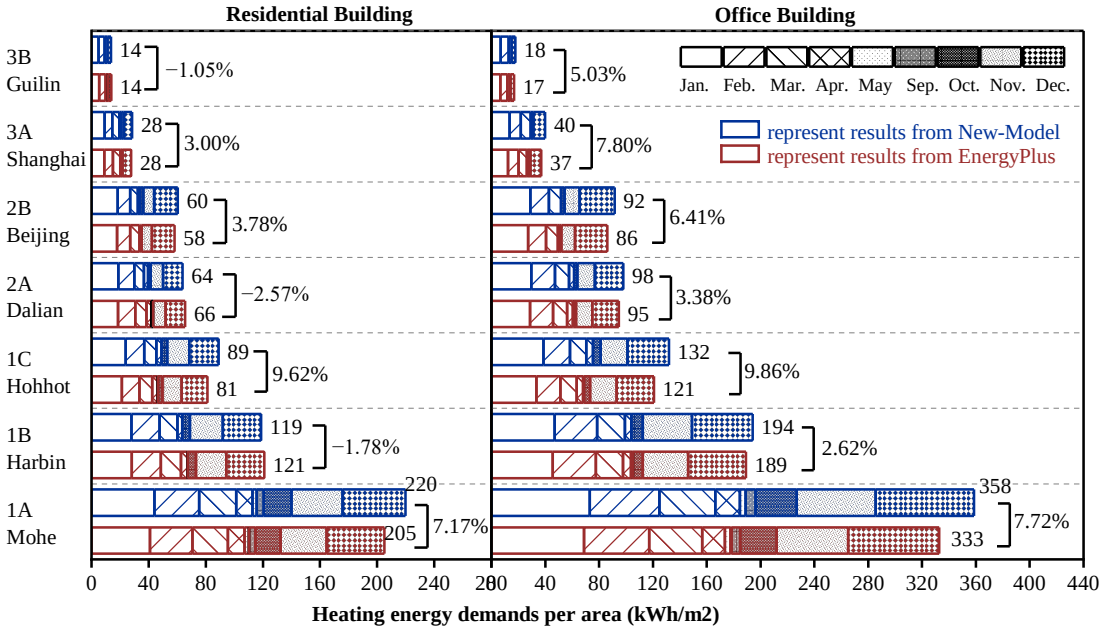

Figure 9. Annual heating loads of residential and office buildings in representative cities in different climate zones.

4.4. Performance Evaluation of Building Envelopes for Different Standards and Different Climate Zones

The building model constructed based on the details of the envelope structure given in Table 9 is regarded as the benchmark building. The model built according to the thermophysical parameters stipulated in the current GB 55015-2021, given in Table 10, is regarded as an energy-saving building. The model built according to the thermal technical parameters specified in GB/T 51350-2019, given in Table 10, is regarded as the NZEBs. Under three different thermal engineering design requirements, a statistical analysis was conducted on the annual heating loads per unit area of all investigated cities in different climate zones in Figure 6, and the results are shown in Figure 10.

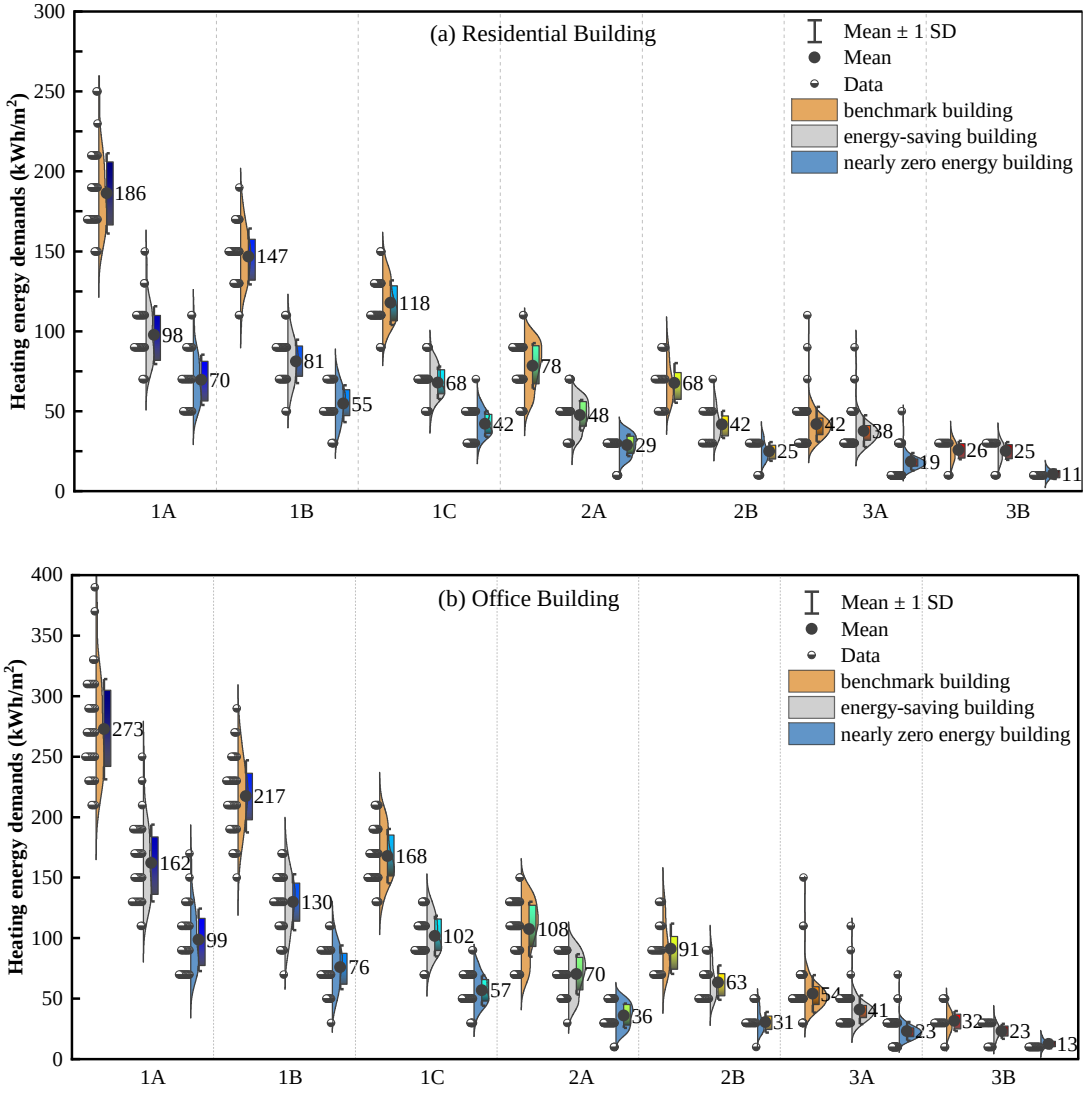

Figure 10. Distribution of annual heating loads for (**a**) residential buildings and (**b**) office buildings built according to different standards.

Taking the energy-saving building as an example, the average value and standard deviation of annual heating loads per unit area for residential buildings from 1A to 3B climate zones are 98 ± 18, 81 ± 14, 68 ± 10, 48 ± 10, 42 ± 9, 38 ± 9, and 25 ± 6 kWh/m^2. The corresponding values for office buildings are 162 ± 32, 130 ± 23, 102 ± 17, 70 ± 17, 63 ± 14, 41 ± 12, and 23 ± 6 kWh/m^2. Under the same building energy efficiency standard scheme, the heat load of office buildings in the same climate zone is significantly higher than that of residential buildings. One of the reasons, as can be seen from Table 10, is that the thermal performance requirements of the residential building envelopes are more stringent. In comparing the annual heat loads of the residential building case in this study with the corresponding value of new residential buildings in different climate zones stipulated in *GB 55015-2021* [15] of China, we can see that the calculation results calculated in this study are large. The main reason is that the model established in this study is based on a single-zone model, and the heating setpoint temperature of all rooms is 21 °C. Future work could focus on real room functions and corresponding indoor setpoint temperatures.

Moreover, the statistical results in Figure 10 show that under different thermal design parameters, there are considerable differences in the energy performance indicators that represent the building heat loads. Taking energy-saving residential buildings as an example, compared with benchmark buildings, the reduction rates of building energy intensity (annual

heat loads per unit area) in climate zones 1A to 3B are 48%, 45%, 42%, 39%, 38%, 10%, and 2% respectively. Nearly zero-energy residential buildings in different climate zones can further reduce building energy intensity by 29, 32, 38, 39, 40, 51, and 58% based on energy-saving residential buildings. The average heating energy intensity of NZEBs across climate zones was reduced by approximately 61% compared to the benchmark building. From the calculated data, it is clear that by improving the thermal performance of the building envelopes, the energy-saving rate of the building itself can reach around 60%. It is a common finding that the improvement in the thermal performance and airtightness of the building envelope can lead to a high level of energy savings for the building itself [56,57]. However, some studies [50] have also pointed out that calculations based on the single-zone model, even after taking into account the correction for intermittent heating, still result in an overestimation of energy savings. Moreover, some research [58] argues that simplified single-zone models deviated negligibly from detailed multi-zone models. Further work would focus on the development of the multi-thermal zone model to obtain the calculation results to choose the suitable model for research purposes. The same analysis was conducted on the office building cases. It is observed that compared with the benchmark building, the energy-saving office buildings constructed based on the current energy-efficient codes have reduced building heat loads by 41, 40, 39, 35, 31, 24, and 26%, respectively. Then, based on energy-saving buildings, the office building energy intensity of NZEBs has been further reduced by 39, 41, 44, 49, 52, 44, and 46%. Additionally, it can be seen from the data distribution of the violin plot in Figure 10 that with more stringent thermal design requirements for building envelopes, the distribution range of heating energy demand of cities in the same climate zone becomes smaller. This means that under stricter thermal design regulations, the differences in the heating energy performance indicators of buildings with the same climate characteristics are spread out over a narrower range, which is beneficial to energy managers. The obtained conclusion of annual heat loads can be applied to energy management in the building planning stage.

In the process of calculating building heating energy demand, an important intermediate parameter is the building balance point temperature, which is of considerable significance for judging whether a building requires auxiliary mechanical heating under certain weather conditions. According to the heat transfer coefficient values given in Section 4.3, the monthly building balance point temperatures were calculated for each city under different thermal performance requirements. Then, we took the average value of each heating month using the criterion $0 \leq \gamma_m \leq 2$ as the heating balance point temperature of this area.

Through the calculation of the residential building, the balance point temperatures of multi-story houses in different cities were obtained as shown in Figure 11a, and statistical analysis was conducted based on different climate zones. Considering all surveyed cities in the same climate zone, taking energy-saving residential buildings as an example, the average and standard deviations of the balance point temperature in each climate zone were 11 ± 2, 11 ± 2, 12 ± 2, 13 ± 1, 13 ± 1, 16 ± 1, and 16 ± 1 °C. Clearly from climate zones 1A to 3B, the balance point temperature of residential buildings showed an overall upward trend. This is because in the thermal engineering standards of China, the warmer the climate, the lower the thermal performance requirements for the building envelopes, that is, the greater the heat transfer coefficients. Under the thermal design requirements of the envelope stipulated by the three building standard schemes, the statistical results of the heating balance point temperature of office buildings in each climate zone are shown in Figure 11b. Taking energy-saving office buildings as an example, the average and standard deviation of balance point temperature of the office buildings in 1A to 3B are 8 ± 2, 9 ± 1, 9 ± 1, 10 ± 1, 11 ± 1, 13 ± 1, and 14 ± 1 °C, respectively. As the thermal insulation performance of the envelope decreased, the building balance point shows an overall upward trend, gradually approaching the indoor design set point. The obtained conclusions are consistent with Harvey [29] and Park [34]. The focus of this study is not on the factors affecting the balance point temperature, which has been discussed in our previous research [33]. In this study, statistics were made on the heating balance point

temperature under different thermal performances in different climate zones in China. Future work could use it as base temperatures to calculate heating degree days, which can be used for climate zoning research based on building performance.

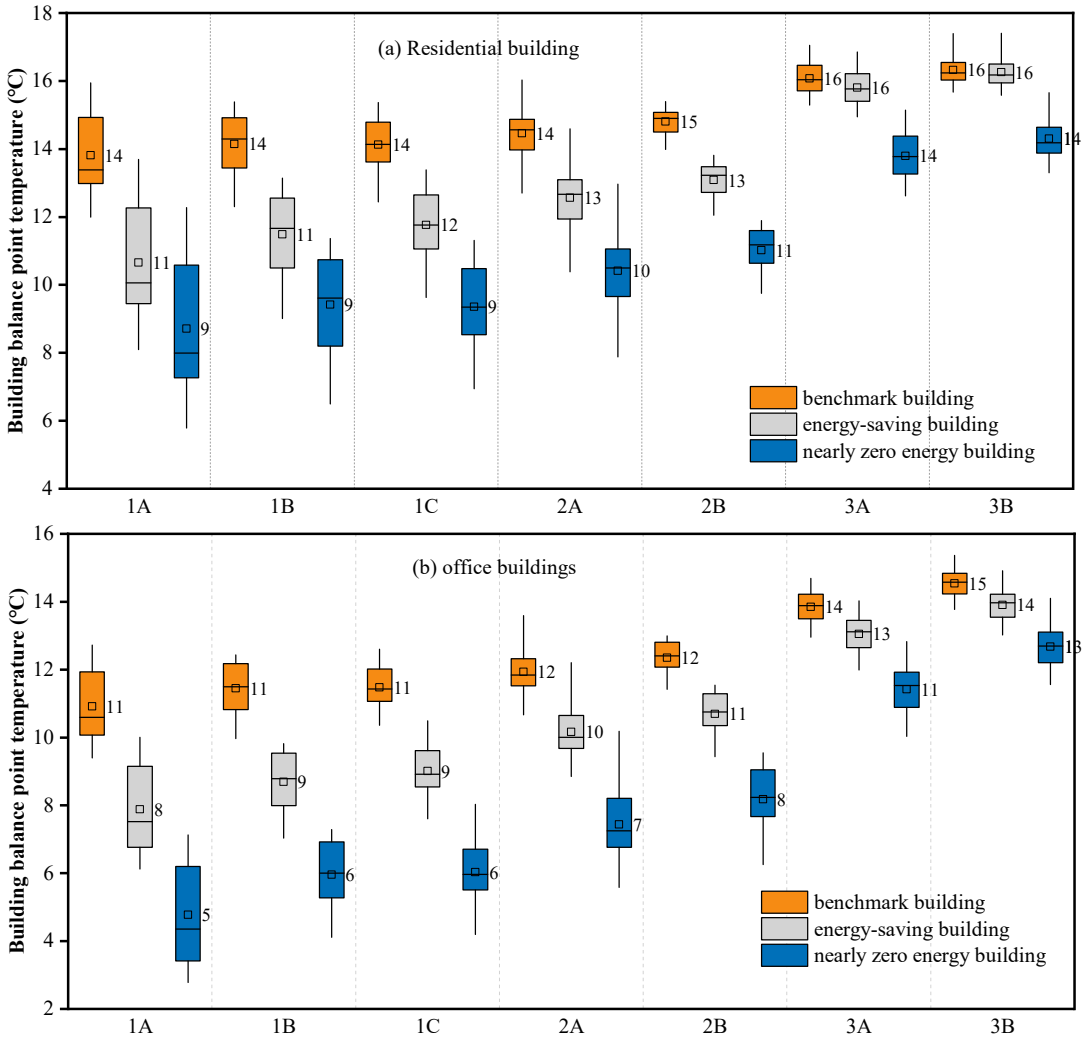

Figure 11. Building balance point temperatures in different climate zones (**a**) residential building; (**b**) office building.

Further comparative analysis was made on the balance point temperature of residential and office buildings under different thermal design requirements. Taking the severe cold zone 1A as an example, from the benchmark buildings constructed in the 1980s to the current energy-saving buildings, and then to the NZEBs, the balance point temperature of the typical residential building constructed in this study dropped from 14 to 11 °C and further decreased to 9 °C. The balance point temperature for the typical office building dropped from 11 to 8 °C and down to 5 °C. This indicates that for residential buildings located in severe cold zone 1A, an auxiliary mechanical heating system is required for buildings built in the 1980s when the outdoor air temperature is below 14 °C. Energy-saving residential buildings require auxiliary heating systems when the outdoor air temperature is below 11 °C. In NZEBs, the mechanical heating systems are only required to be turned on when the outdoor air temperature is lower than 9 °C. Compared with residential buildings, the balance point temperature of office buildings is lower, which means that when the indoor setpoint temperature of residential and office buildings is the same, office buildings should turn on the mechanical heating systems for a shorter period throughout the year. This finding is due to the hypothesis that there are more internal heat gains in the office building, which causes a temperature rise in the building to maintain its indoor temperature.

Then, the reason for the high heat load of the office buildings in Figure 10 is that the heat loss caused by heat transfer and infiltration of the office building envelopes is greater than that of residential buildings.

In Figure 12, the relationships between the annual heating loads vs. HDD18 are further reported for all surveyed cities in climate zones 1A, 2A, and 3A. The left side of the figures represents office buildings, whereas the right side represents residential buildings. The three solid lines or dashed lines in each panel are, moving upward, best-fit lines for NZEBs, energy-saving buildings, and benchmark buildings, respectively. The HDD18 of each city is generally directly given in Chinese National Standard, ASHRAE, and other standards. As a commonly used independent variable, its value is generally considered to have a satisfactory linear correlation with the heating energy demand. However, we found that this is not the case through a linear regression analysis of annual heating energy demand and HDD18. For severe cold zone 1A, under the current energy efficiency code and nearly zero energy building technical standard, the coefficient of determination R^2 was almost below 0.5, which means that HDD18 explains less than 50% of the heating energy use for energy-saving buildings and NZEBs. The same analysis was conducted for the cold zone 2A and it was observed that HDD18 explains less than 90% of the heating energy demand under the current energy efficiency standard scheme. Although this correlation is not low, the stricter the standard, the lower the actual base temperature of the building (compared to the current base temperature of 18 °C), and the worse the correlation between HDD18 and heat load. Notably, a good correlation between heating energy requirements vs. HDD18 was observed, with R^2 almost higher than 0.95, in hot summer and cold winter zone 3A. Such a result may be owing to the higher heating balance point temperature of residential and office buildings in the hot summer and cold winter zone, which is close to the current base temperature of 18 °C.

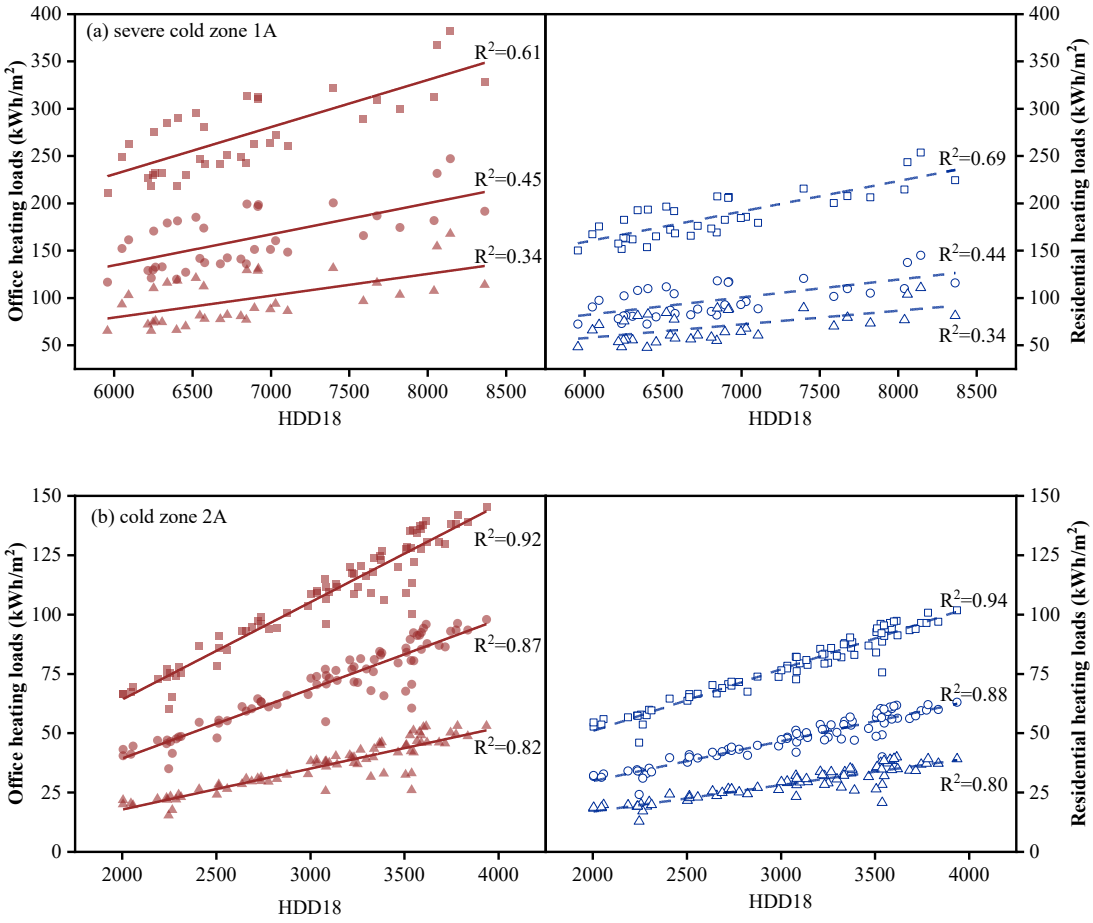

Figure 12. *Cont.*

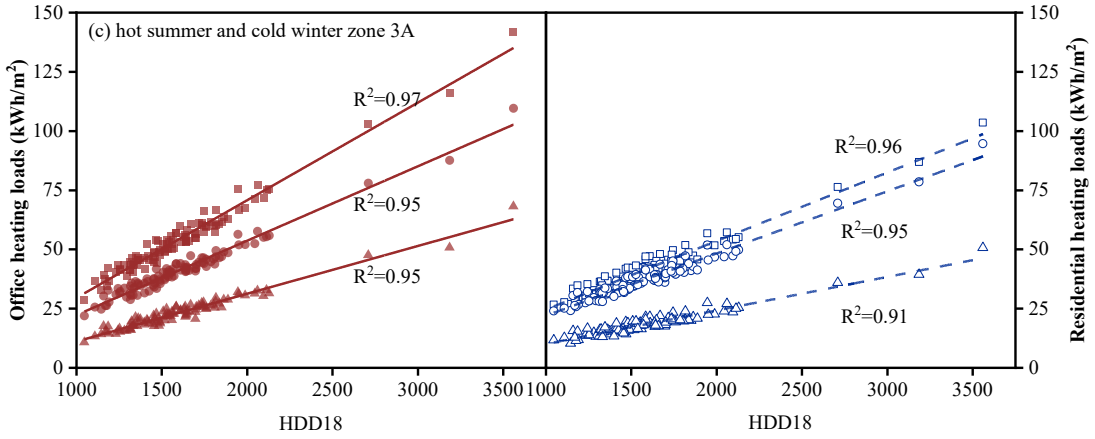

Figure 12. Annual heating loads vs. HDD18 in different climate zones.

In conclusion, HDDs are a good explanation for heating loads when their base temperature coincides with the balance point temperature. Conversely, when there is a large difference between the selected base temperature and the building balance point temperature, HDD explains less about the annual heating loads. This further demonstrates that HDDs in different climate zones should be recalculated based on the appropriate base temperature instead of using the current HDD18.

5. Conclusions

In this study, we calculated the monthly heating balance point temperature of the building based on the quasi-steady-state method provided by ISO 52016 and determined it as the base temperature to predict building heating energy demand using the variable-base degree-day method. Based on the above calculation procedure, a building performance evaluation tool BPT V1.0 was developed, which provides a quick estimation of the annual heat loads in any city with heating demand. Through the validation tests and case studies of BPT V1.0, several conclusions can be drawn.

- The algorithm of the BPT V1.0 program can well reflect the influence of particular heat transfer processes and different physical phenomena on the results of building heating energy demand, such as thermal mass, internal gains, infiltration, setback thermostat control, exterior solar absorptance, south solar gains, and window orientation. By analyzing the cases of residential and office buildings in different climate zones, and comparing the calculation results with the energy simulation software EnergyPlus, the adaptability of BPT V1.0 under different climatic conditions is further proved.
- The simplified model established in this study can accurately calculate the heating energy demand of buildings based on the thermophysical parameters of the building envelope and the TMY data of the investigated cities. It can provide a reference for energy managers and a basis for estimating the building energy efficiency performance with different envelope thermal properties in the region. Taking the current building energy-efficiency code as an example, the average annual heating loads per unit area of residential buildings from climate zones 1A to 3B were 98, 81, 68, 48, 42, 38, and 25 kWh/m^2, and the corresponding values for office buildings were 162, 130, 102, 70, 63, 41, and 23 kWh/m^2, respectively. From energy-saving buildings to NZEBs, the energy efficiency of residential buildings in different climate zones improved by 29, 32, 38, 39, 40, 51, and 58%, respectively. The energy efficiency of office buildings increased by 39, 41, 44, 49, 52, 44, and 46%, respectively.
- We analyzed the balance point temperature of residential and office buildings under different thermal performance requirements and found that the balance point temperature decreased with the improvement in building thermal performance. This means that under the same climatic conditions, the period that the nearly-zero energy buildings need auxiliary mechanical heating throughout the year is shortened.

From the severe cold zone to the hot summer and cold winter of China, the balance point temperature of residential buildings built according to the current standard *GB 55015-2021* ranges from 11 to 16 °C and 8 to 14 °C for office buildings.

- It is advisable to recalculate the HDDs using the monthly building balance point temperature as the variable base temperature, particularly in severe cold regions. As the currently commonly used HDD18 explains less than 50% of the heating energy demand of current energy-saving buildings and nearly zero-energy buildings, evidently, with the implementation of more stringent building thermal regulations, the HDD values given in current standards should be updated regularly in the future.

In the near future, with the help of BPT V1.0, the analysis and the optimization of several building strategies, such as window-to-wall ratio, orientation, envelope insulation, airtightness, etc., could be carried out at the early stage of design for building energy efficiency. The model developed in this study is mainly used to predict building heat loads in the planning stage. To simplify calculations, the current model is based on a single-thermal zone model to calculate energy needs under the same interior design conditions. Improvements to the model could be performed, such as adding shading analysis, multiple-thermal zone coupling calculations, etc., and additional modeling capabilities and validations could be included in the code, such as procedures related to latent heat loads and cooling loads calculations.

Author Contributions: Conceptualization, Z.H. and J.X.; methodology, Z.H.; software, Z.H.; validation, Z.H. and X.Z.; formal analysis, Z.H.; investigation, Z.H.; resources, J.L.; data curation, Z.H.; writing—original draft preparation, Z.H.; writing—review and editing, Z.H., J.X. and X.Z.; visualization, Z.H.; supervision, J.L.; project administration, J.X.; funding acquisition, J.X. All authors have read and agreed to the published version of the manuscript.

Funding: This research was funded by the Key Program of the National Natural Science Foundation of China (No. 51838011) and the General Program of the National Natural Science Foundation of China (No. 52178061).

Data Availability Statement: The data presented in this study are available on request from the corresponding author. The data are not publicly available due to local policies.

Conflicts of Interest: Authors declare that there are no financial or personal relationships with other people or organizations that can inappropriately influence our work, and there is no professional or other personal interest of any nature or kind in any product, service, and/or company that could be constructed as influencing the position presented in, or the review of, the manuscript entitled "Simplified model of heat load prediction and its application in estimation of building envelope thermal performance".

References

1. Méndez Echenagucia, T.; Capozzoli, A.; Cascone, Y.; Sassone, M. The early design stage of a building envelope: Multi-objective search through heating, cooling and lighting energy performance analysis. *Appl. Energy* **2015**, *154*, 577–591. [CrossRef]
2. Luo, Y.; Zhang, L.; Liu, Z.; Yu, J.; Xu, X.; Su, X. Towards net zero energy building: The application potential and adaptability of photovoltaic-thermoelectric-battery wall system. *Appl. Energy* **2020**, *258*, 114066. [CrossRef]
3. Cornaro, C.; Basciano, G.; Puggioni, V.A.; Pierro, M. Energy Saving Assessment of Semi-Transparent Photovoltaic Modules Integrated into NZEB. *Buildings* **2017**, *7*, 9. [CrossRef]
4. Liu, Z.; Liu, Y.; He, B.-J.; Xu, W.; Jin, G.; Zhang, X. Application and suitability analysis of the key technologies in nearly zero energy buildings in China. *Renew. Sustain. Energy Rev.* **2019**, *101*, 329–345. [CrossRef]
5. MoHURD. *Building Energy Conservation and Green Building Development 14th Five-Year Plan*; Ministry of Housing and Urban-Rural Development Website: Beijing, China, 2022.
6. Xing, R.; Hanaoka, T.; Kanamori, Y.; Masui, T. Achieving zero emission in China's urban building sector: Opportunities and barriers. *Curr. Opin. Environ. Sustain.* **2018**, *30*, 115–122. [CrossRef]
7. Passive House Institute. Criteria for the Passive House, EnerPHit and PHI Low Energy Building Standard. 2015. Available online: https://passiv.de/downloads/03_building_criteria_en.pdf (accessed on 15 April 2023).
8. Sharma, S.K. Zero Energy Building Envelope Components: A Review. *Int. J. Eng. Res. Appl.* **2013**, *3*, 662–675.
9. Lin, Y.; Zhong, S.; Yang, W.; Hao, X.; Li, C.-Q. Towards zero-energy buildings in China: A systematic literature review. *J. Clean. Prod.* **2020**, *276*, 123297. [CrossRef]

10. IEA. *Building Envelopes*; IEA: Paris, France, 2022; License: CC BY 4.0.
11. Bhardwaj, M.; Arora, A. Designs of Building Envelopes with Improved Energy Efficiency. In *Emerging Trends in Energy Conversion and Thermo-Fluid Systems: Select Proceedings of iCONECTS 2021*; Springer Nature: Singapore, 2022; pp. 191–203.
12. Deb, C.; Gelder, L.V.; Spiekman, M.; Pandraud, G.; Jack, R.; Fitton, R. Measuring the heat transfer coefficient (HTC) in buildings: A stakeholder's survey. *Renew. Sustain. Energy Rev.* **2021**, *144*, 111008. [CrossRef]
13. Sassine, E.; Kinab, E.; Cherif, Y.; Antczak, E.; Nasrallah, M. Thermal performance of lightweight concrete applications in building envelopes in Lebanon. *Build. Simul.* **2021**, *14*, 1359–1375. [CrossRef]
14. MoHURD. *Design Standard for Energy Efficiency of Residential Buildings in Severe Cold and Cold Zones*; China Architecture Publishing and Media Co., Ltd.: Beijing, China, 2018.
15. MoHURD. *General Code for Energy Efficiency and Renewable Energy Application in Buildings*; China Architecture Publishing and Media Co., Ltd.: Beijing, China, 2021; Volume GB 55015-2021, p. 115.
16. *GB/T 51350-2019*; CABR; HABR. Technical Standard for Nearly Zero Energy Buildings. China Architecture Publishing and Media Co., Ltd.: Beijing, China, 2019; p. 126.
17. Abu Bakar, N.N.; Hassan, M.Y.; Abdullah, H.; Rahman, H.A.; Abdullah, M.P.; Hussin, F.; Bandi, M. Energy efficiency index as an indicator for measuring building energy performance: A review. *Renew. Sustain. Energy Rev.* **2015**, *44*, 1–11. [CrossRef]
18. Boemi, S.-N.; Tziogas, C. Indicators for Buildings' Energy Performance. In *Energy Performance of Buildings: Energy Efficiency and Built Environment in Temperate Climates*; Boemi, S.-N., Irulegi, O., Santamouris, M., Eds.; Springer International Publishing: Cham, Switzerland, 2016; pp. 79–93. [CrossRef]
19. Martínez-de-Alegría, I.; Río, R.-M.; Zarrabeitia, E.; Álvarez, I. Heating demand as an energy performance indicator: A case study of buildings built under the passive house standard in Spain. *Energy Policy* **2021**, *159*, 112604. [CrossRef]
20. Shanqin, Y. Estimation of Heating Heat Consumption and Building Energy Saving Design Using Effective Heat Transfer Coefficient Method. *Build. Sci.* **1986**, *2*, 55–65.
21. Shuai, Z.; Yan, L.; Liqiang, H.; Jiang, L.; Liu, Y. Comparative study on energy efficiency calculation methods of residential buildings in central heating areas of Northern China. *J. Harbin Inst. Technol.* **2019**, *51*, 178–185.
22. Michalak, P. A thermal network model for the dynamic simulation of the energy performance of buildings with the time varying ventilation flow. *Energy Build.* **2019**, *202*, 109337. [CrossRef]
23. Javanroodi, K.; Nik, V.M. Impacts of Microclimate Conditions on the Energy Performance of Buildings in Urban Areas. *Buildings* **2019**, *9*, 189. [CrossRef]
24. Kotarela, F.; Kyritsis, A.; Agathokleous, R.; Papanikolaou, N. On the exploitation of dynamic simulations for the design of buildings energy systems. *Energy* **2023**, *271*, 127002. [CrossRef]
25. Hong, T.; Langevin, J.; Sun, K. Building simulation: Ten challenges. *Build. Simul.* **2018**, *11*, 871–898. [CrossRef]
26. *ISO 52016-1:2017*; Energy Performance of Buildings—Energy Needs for Heating and Cooling, Internal Temperatures and Sensible and Latent Heat Loads—Part 1: Calculation Procedures. ISO: Geneva, Switzerland, 2022; p. 204.
27. Zhenyu, Y.; Xu, W.; Zou, Y.; Deyu, S. Comparison between quasi-steady energy calculation software IBE and dynamic simulation software TRNSYS applied to cold zone. *Heat. Vent. Air Cond.* **2018**, *48*, 107–113.
28. Committees, A.T. 2021 ASHRAE Handbook—Fundamentals, Chapter: Energy Estimating and Modeling Methods. In *2005 ASHRAE Handbook: Fundamentals*; American Society of Heating, Refrigeration, and Air-Conditioning Engineers (ASHRAE): Peachtree Corners, GA, USA, 2021.
29. Harvey, L.D.D. Using modified multiple heating-degree-day (HDD) and cooling-degree-day (CDD) indices to estimate building heating and cooling loads. *Energy Build.* **2020**, *229*, 110475. [CrossRef]
30. Meng, Q.; Xi, Y.; Zhang, X.; Mourshed, M.; Hui, Y. Evaluating multiple parameters dependency of base temperature for heating degree-days in building energy prediction. *Build. Simul.* **2021**, *14*, 969–985. [CrossRef]
31. Utzinger, M.; Wasley, J.H. *Vital Signs: Building Balance Point*; Vital Signs Curriculum Materials Project; University of California–Berkeley: Berkeley, CA, USA; University of Wisconsin: Milwaukee, WI, USA, 1997.
32. Cheng, X.; Li, S. Interval Estimations of Building Heating Energy Consumption using the Degree-Day Method and Fuzzy Numbers. *Buildings* **2018**, *8*, 21. [CrossRef]
33. Hao, Z.; Zhang, X.; Xie, J.; Yin, K.; Liu, J. Balance point temperature and heating degree-days in different climate conditions for building energy efficiency applications. *Build. Environ.* **2022**, *216*, 109013. [CrossRef]
34. Park, S.; Shim, J.; Song, D. Issues in calculation of balance-point temperatures for heating degree-days for the development of building-energy policy. *Renew. Sustain. Energy Rev.* **2021**, *135*, 110211. [CrossRef]
35. Ren, J.; Wu, J. Calculating Residential Heat Consumption Using Variable-Base Degree Days. *Heat. Vent. Air Cond.* **1992**, *4*, 9–11+21. Available online: http://qikan.cqvip.com/Qikan/Article/Detail?id=1005159695 (accessed on 15 April 2023).
36. *ISO 13789:2017*; Thermal Performance of Buildings—Transmission and Ventilation Heat Transfer Coefficients—Calculation Method. ISO: Geneva, Switzerland, 2017.
37. Nielsen, T.R.; Duer, K.; Svendsen, S. Energy performance of glazings and windows. *Sol. Energy* **2001**, *69*, 137–143. [CrossRef]
38. Karlsson, J.; Roos, A. Modelling the angular behaviour of the total solar energy transmittance of windows. *Sol. Energy* **2000**, *69*, 321–329. [CrossRef]
39. Urbikain, M.K.; Sala, J.M. Analysis of different models to estimate energy savings related to windows in residential buildings. *Energy Build.* **2009**, *41*, 687–695. [CrossRef]

40. Büyükalaca, O.; Bulut, H.; Yılmaz, T. Analysis of variable-base heating and cooling degree-days for Turkey. *Appl. Energy* **2001**, *69*, 269–283. [CrossRef]
41. Wortman, D.; Christensen, C. Variable-base degree-day correction factors for energy savings calculations. *ASHRAE Trans.* **1985**, *91*, 934–944.
42. Hitchin, E.R. Estimating monthly degree-days. *Build. Serv. Eng. Res. Technol.* **1983**, *4*, 159–162. [CrossRef]
43. Schito, E.; Testi, D.; Conti, P.; Grassi, W. Validation of Seas, a Quasi-Steady-State Tool for Building Energy Audits. *Energy Procedia* **2015**, *78*, 3192–3197. [CrossRef]
44. ANSI/ASHRAE. Standard Method Of Test For The Evaluation Of Building Energy Analysis Computer Programs. In *ANSI/ASHRAE Standard 140-2017*; American Society of Heating, Refrigerating and Air-Conditioning Engineers, Inc.: Peachtree Corners, GA, USA, 2017.
45. Neymark, J.; Judkoff, R.; Knabe, G.; Le, H.T.; Dürig, M.; Glass, A.; Zweifel, G. Applying the building energy simulation test (BESTEST) diagnostic method to verification of space conditioning equipment models used in whole-building energy simulation programs. *Energy Build.* **2002**, *34*, 917–931. [CrossRef]
46. Melo, A.P.; Cóstola, D.; Lamberts, R.; Hensen, J.L.M. Assessing the accuracy of a simplified building energy simulation model using BESTEST: The case study of Brazilian regulation. *Energy Build.* **2012**, *45*, 219–228. [CrossRef]
47. Buonomano, A.; Palombo, A. Building energy performance analysis by an in-house developed dynamic simulation code: An investigation for different case studies. *Appl. Energy* **2014**, *113*, 788–807. [CrossRef]
48. Judkoff, R.; Neymark, J. *The BESTEST Method for Evaluating and Diagnosing Building Energy Software*; American Council for an Energy-Efficient Economy: Washington, DC, USA, 1998.
49. Zhang, X.; Qu, Y.; Li, H. Study on the Model Parameters of Monthly Energy Balance Method for Ultra-low Energy Buildings. *Build. Energy Environ.* **2021**, *40*, 1–6.
50. Delghust, M.; De Weerdt, Y.; Janssens, A. Zoning and Intermittency Simplifications in Quasi-steady State Models. *Energy Procedia* **2015**, *78*, 2995–3000. [CrossRef]
51. Wauman, B.; Breesch, H.; Saelens, D. Evaluation of the accuracy of the implementation of dynamic effects in the quasi steady-state calculation method for school buildings. *Energy Build.* **2013**, *65*, 173–184. [CrossRef]
52. Chen, Y.; Guo, M.; Chen, Z.; Chen, Z.; Ji, Y. Physical energy and data-driven models in building energy prediction: A review. *Energy Rep.* **2022**, *8*, 2656–2671. [CrossRef]
53. Al-janabi, A.; Kavgic, M.; Mohammadzadeh, A.; Azzouz, A. Comparison of EnergyPlus and IES to model a complex university building using three scenarios: Free-floating, ideal air load system, and detailed. *J. Build. Eng.* **2019**, *22*, 262–280. [CrossRef]
54. D'Amico, A.; Ciulla, G.; Panno, D.; Ferrari, S. Building energy demand assessment through heating degree days: The importance of a climatic dataset. *Appl. Energy* **2019**, *242*, 1285–1306. [CrossRef]
55. *JGJ/T346-2014*; CABR; XAUAT. Standard for Weather Data of Building Energy Efficiency. China Architecture Publishing & Media Co., Ltd.: Beijing, China, 2015.
56. Daouas, N. A study on optimum insulation thickness in walls and energy savings in Tunisian buildings based on analytical calculation of cooling and heating transmission loads. *Appl. Energy* **2011**, *88*, 156–164. [CrossRef]
57. Bolattürk, A. Optimum insulation thicknesses for building walls with respect to cooling and heating degree-hours in the warmest zone of Turkey. *Build. Environ.* **2008**, *43*, 1055–1064. [CrossRef]
58. Johari, F.; Munkhammar, J.; Shadram, F.; Widén, J. Evaluation of simplified building energy models for urban-scale energy analysis of buildings. *Build. Environ.* **2022**, *211*, 108684. [CrossRef]